ISSN 2706-655X Vol.5, Issue 3: 16-25, DOI: 10.25236/IJFET.2023.050304

CFD simulation analysis of aerodynamic characteristics of large wind turbine unit under accident condition

Guo Li

School of Mechanical Engineering, Hunan University of Science and Technology, Xiangtan, China

Abstract: *In this paper, according to different locations of blade fracture accidents, it is divided into three fractures: blade root fracture, leaf middle fracture and blade tip fracture. Assuming that the blade fracture accident due to aging is operated at the rated wind speed and rated speed, CFD simulation is carried out to analyze the wind rotation field, aerodynamic load and blade surface streamline characteristics of NREL 5MW wind turbine with different fracture positions. This paper also assumes that under the condition of a strong typhoon, the instantaneous wind speed is too large, resulting in the wind turbine speeding, and then the blade fracture accident occurs. At this time, the wind turbine was running under extreme wind speeds, and the speed soared due to the speeding car. Analyze aerodynamic loads at different speeds. It provides an important reference for the design and operation and maintenance of wind turbine blades.*

Keywords: *Wind turbine accident; Blade fracture; Aerodynamic characteristics; CFD simulation*

1. Introduction

Blade accident is one of the most common accidents in wind farms. Due to the change of wind speed and direction, the wind turbulence environment temperature change, solar radiation, rain, hail, snow and ice, as well as storm, lightning, dust storm, salt fog, sub-freezing period and other external adverse environmental stresses, the load on the wind turbine blade is complex and variable. The long-term impact of these complex and variable loads is easy to damage the blades. Therefore, the blade usually lasts for less than 20 years of its typical design life, and there are potential serious problems, such as blade root fracture, blade fracture, blade edge fracture and peeling, glue opening and other problems. When a blade fails, it will cause the unit to vibrate violently and may cause the whole unit to fail.

Therefore, experts and scholars at home and abroad have carried out many studies on accidents such as blade fracture, Chou et al [1] The mechanical mechanism of wind turbine tower collapse and blade fracture is studied, and the mechanical analysis is carried out by finite element method to determine the failure mechanism and structural weak surface, so as to support the future risk prevention and anti-risk design of wind turbine. Chen et al [2] The structural failure of wind turbine damaged by strong typhoon is studied. It is found that the possible root cause of blade fracture is that the blade strain exceeds the failure strain of unidirectional composite material in the flange strip of the wing beam, and the blade failure occurs at the normalized blade length of about 0.26 to 0.48. Dai[3] The wind turbine load model is established in the Simulink environment, and it is assumed that a blade is completely broken from the root, and the wind turbine still does not stop within a few seconds after the blade breaks. Through simulation research, it is found that after a blade breaks, the rotating torque of the wind turbine will suddenly change, the speed of the wind turbine will fluctuate near the control set point, and the wind turbine capacity will be captured and converted in imbalance. Han et al [4] Through the observation and analysis of the accident parts of the blade root fracture, it is determined that the low cycle fatigue of the blade is due to the problems in the process control during the production process, resulting in the incomplete curing of the local resin at the blade root, resulting in the low strength and stiffness of the area. When the concentrated load is received, the stress concentration occurs, the first delamination cracking occurs, and finally the fracture occurs. He et.al [5] Taking a small wind turbine as an example, a three-dimensional model of the wind turbine's fluid and solid computational domain is established for two cases: the blade is intact and a third of the blade tip is broken, and the unidirectional fluid-structure coupling is carried out. Gu et al. [6] through finite element simulation, it is found that the middle and root of the blade are more prone to break than other positions, and the suddenly broken blade will cause stress concentration at the root of other blades.

ISSN 2706-655X Vol.5, Issue 3: 16-25, DOI: 10.25236/IJFET.2023.050304

To sum up, at present, in the field of blade fracture accidents, the research mainly focuses on the analysis of fracture causes and mechanical load, and has achieved certain research results. Some research has good guiding value for the production and maintenance of wind turbine blades. However, there are relatively few studies on the flow field of wind turbine when the blade breaks at different positions.For this reason, the flow field simulation analysis of the wind turbine under different blade fracture accidents is carried out in this paper, and the multi-speed simulation is also carried out for the fracture caused by the flying car under the failure of emergency pitching to analyze its aerodynamic load changes.

2. Blade structure and calculation method

2.1. Blade structure under accident condition

The accident state studied in this paper is blade fracture. In order to facilitate the study, the blade fracture forms are divided into blade root fracture, blade middle fracture and blade tip fracture. The blade structure under these three fracture states is shown in Figure 1. Blade 1 is the broken blade, Blade 2 is the first blade close to the broken blade in the direction of rotation, and Blade 3 is the second blade close to the broken blade in the direction of rotation.

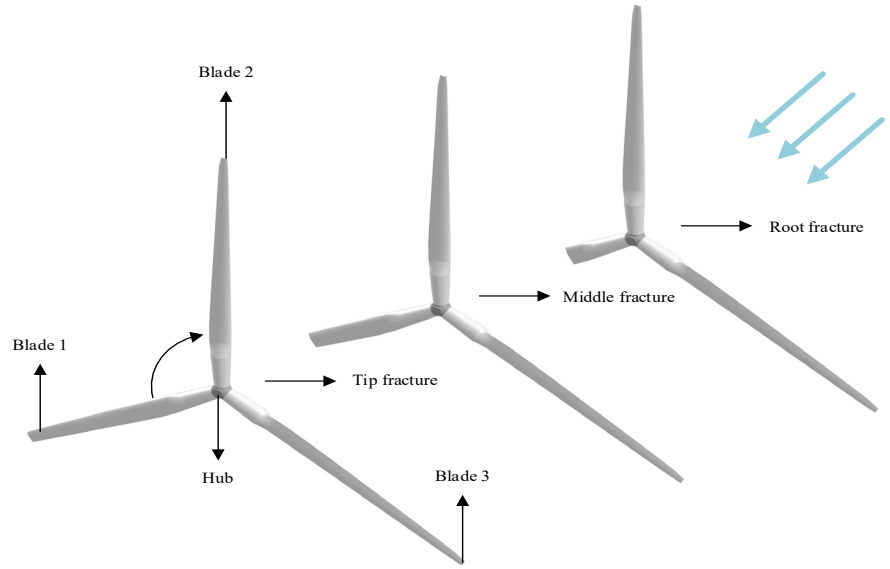

Figure 1: Blade fracture structure

2.2. CFD analysis method

CFD is realized by solving the Navier-Stokes equation of fluid mechanics in a numerical discrete way. At present, the commonly used numerical simulation methods include Reynolds mean (RANS), large eddy simulation (LES), hybrid RANS/LES method and direct numerical simulation (DNS). In this paper, the fluid in the case of blade fracture is considered as stable and incompressible. RANS method and SST k-turbulence model are used for numerical calculation. The governing equation of stable incompressible flow is as follows

$$\frac{\partial \overline{u}_i}{\partial x_i} = 0 \tag{1}$$

$$\rho \frac{\partial (\rho \overline{u}_i \overline{u}_j)}{\partial x_i} = -\frac{\partial \overline{p}}{\partial x_i} + \frac{\partial}{\partial x_i}\left[\mu\left(\frac{\partial \overline{u}_i}{\partial x_j} + \frac{\partial \overline{u}_j}{\partial x_i}\right) - \rho \overline{u_i' u_j'}\right] \tag{2}$$

Here $\overline{u}_i$ is the velocity value, u_i' is the fluctuation, and $-\rho \overline{u_i' u_j'}$ is the Reynolds stress tension. The Reynolds stress calculation model used is

ISSN 2706-655X Vol.5, Issue 3: 16-25, DOI: 10.25236/IJFET.2023.050304

$$-\rho\overline{u_i'u_j'} = \mu_t\left(\frac{\partial \overline{u}_i}{\partial x_j}+\frac{\partial \overline{u}_j}{\partial x_i}\right)-\frac{2}{3}\rho k\delta_{ij}$$

Where μ_t is turbulent viscosity, k is turbulent kinetic energy and δ_{ij} is second-order tensor.

Menter[7] The SST k-ω turbulence model is proposed and improved to become a turbulence mixing model widely used in engineering [8].The model uses a mixing function to combine the k-ε model and the k-ω model. The k-ω model is used near the wall and the modified k-ε model is used outside the boundary layer, which overcomes the dependence of free-flow turbulence. The general control equation of SST k-ω turbulence model is as follows:

$$\frac{\partial(\rho k)}{\partial t}+\frac{\partial(\rho U_i k)}{\partial x_i}=\widetilde{P_k}-\beta^*\rho k\omega+\frac{\partial}{\partial x_i}\left[(\mu+\sigma_k\mu_t)\frac{\partial k}{\partial x_i}\right] \tag{3}$$

$$\frac{\partial(\rho\omega)}{\partial t}+\frac{\partial(\rho U_i\omega)}{\partial x_i}=\alpha\rho S^2-\beta\rho\omega^2+\frac{\partial}{\partial x_i}\left[(\mu+\sigma_\omega\mu_t)\frac{\partial\omega}{\partial x_i}\right]+2(1-F_1)\rho\sigma_{\omega2}\frac{1}{\omega}\frac{\partial k}{\partial x_i}\frac{\partial\omega}{\partial x_i} \tag{4}$$

Here, the mixing function F_1 is defined as follows:

$$F_1=\tanh\left\{\left\{\min\left[\max\left(\frac{\sqrt{k}}{\beta^*\omega y},\frac{500v}{y^2\omega}\right),\frac{4\rho\sigma_{\omega2}k}{CD_{k\omega}y^2}\right]\right\}^4\right\} \tag{5}$$

Here, $CD_{k\omega}=\max\left(2\rho\sigma_{\omega2}\frac{1}{\omega}\frac{\partial k}{\partial x_i}\frac{\partial\omega}{\partial x_i},10^{-10}\right)$, y is the distance near the wall.

Turbulence viscosity is defined as follows:

$$\mu_t=\frac{a_1k\rho}{\max\left(a_1\omega,SF_2\right)} \tag{6}$$

Here S is the strain rate, which F_2 is the second mixed function defined by the following formula:

$$F_2=\tanh\left\{\left[\max\left(\frac{2\sqrt{k}}{\beta^*\omega y},\frac{500\mu}{\rho y^2\omega}\right)\right]^2\right\} \tag{7}$$

The generation term of turbulent kinetic energy P_k is defined as:

$$P_k=\mu_t\frac{\partial U_i}{\partial x_j}\left(\frac{\partial U_i}{\partial x_j}+\frac{\partial U_j}{\partial x_i}\right) \tag{8}$$

$$\widetilde{P_k}=\min\left(P_k,10\cdot\beta^*\rho k\omega\right) \tag{9}$$

Where β^*, β, a_1, σ_k and σ_ω are constant terms, and the complete parameters can be obtained from the original file.

3. Calculation model and verification

3.1. Computing domain and grid division

This study uses the 5MW reference wind turbine designed by the National Renewable Energy Laboratory (NREL) of the United States, and the specific parameters are shown in Table 1. The wind turbine blades are composed of six types of airfoils: DU40, DU35, DU30, DU25, DU21 and NACA64, with different chord lengths and twist angles. Specific parameters in reference[9].The model of full size NREL 5MW wind turbine is established. In addition, wind turbine models under different fracture

ISSN 2706-655X Vol.5, Issue 3: 16-25, DOI: 10.25236/IJFET.2023.050304

conditions are also established.

Table 1: NREL 5MW parameter table

Turbine parameter	Value
Rated power	5 MW
Rotor diameter	126 m
hub diameter	3 m
Cut-in wind speed	3 m/s
rated wind speed	11.4 m/s
cut-out wind speed	25 m/s
Cut-in speed	6.9 rpm
rated rotor speed	12.1 rpm

Wang et al [10] Select 3R and 10R respectively as the distance from the speed inlet and pressure outlet to the blade, while Ji et al [11] And Abdelgalil et al [12] use 7R as the length from the blade to the pressure outlet (R is the radius of the wind turbine). Therefore, in this paper, the diameter of the velocity inlet is 8R, 3R from the wind wheel, 12R from the pressure outlet, and 7R from the wind wheel, forming a conical calculation domain as shown in Figure 2(a) and (b). Among them, the outer surface of the calculation domain is also considered as the velocity entrance, and its velocity is the same as the main entrance.

As shown in Figure 2(c) and (d), the computational domain is divided into unstructured grids. In order to obtain a better boundary layer solution effect, the expansion layer is applied to the surface of the wind turbine. 15 expansion layers are used, with the expansion rate of 1.5 and the height of the first layer of 4e-5m, so that the y+ value around the whole wind turbine surface is close to 1, as shown in Figure 3.

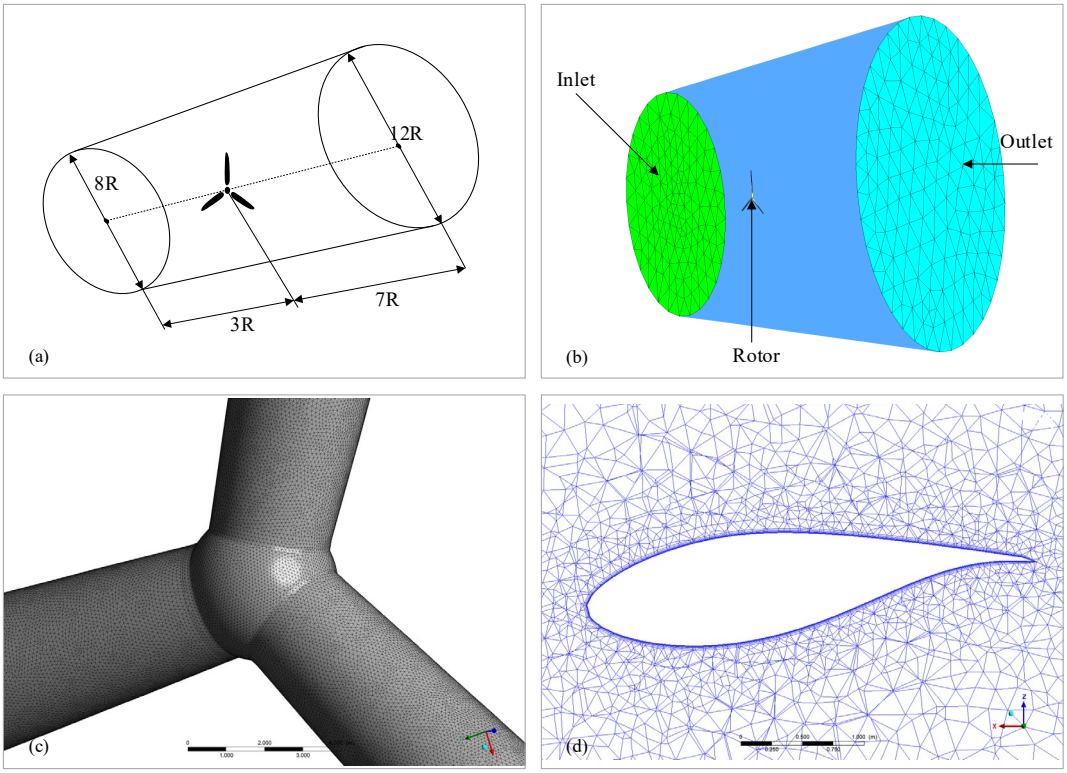

(a) Flow field space settings; (b) Flow field meshing; (c) Blade surface meshing; (d) Local area mesh for wind rotor

Figure 2: Flow field settings of wind rotor

ISSN 2706-655X Vol.5, Issue 3: 16-25, DOI: 10.25236/IJFET.2023.050304

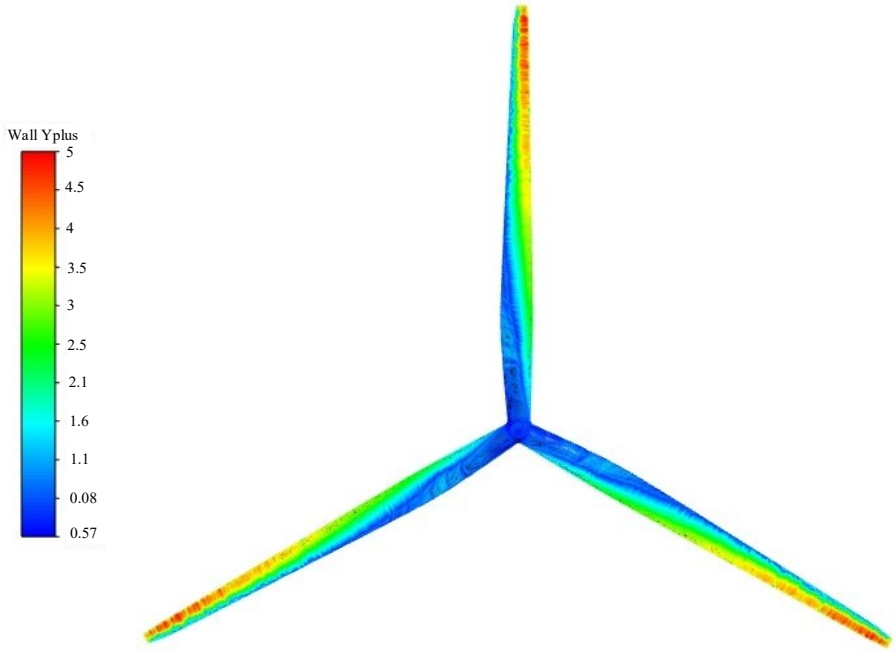

Figure 3: Blade y+ distribution

3.2. Boundary condition

The entrance of the calculation domain is defined as the speed entrance boundary condition with turbulence intensity of 5% and wind speed of 11.4m/s. The outlet is defined as the pressure outlet boundary condition with turbulence intensity of 5%. In this paper, the multi-motion reference system rotation method is adopted. The rotation axis is set as the z-axis, and the rotation speed is set as -1.267rad/s. The wind wheel is defined as a static non-slip wall.

In this paper, three representative blade fracture accident states are used for numerical simulation, including blade root fracture at 25.6% R, blade middle fracture at 52.2% R, and blade tip fracture at 78.9% R. A numerical model is also established for the possible runaway phenomenon after the respective fracture accident. The pressure-velocity coupling scheme is solved by SIMPLE method. The pressure term and momentum term of the control equation are both in second-order discrete format. The corresponding parameter settings remain default. The residual convergence standard is defined as 1e-06, and the number of iterations is set as 1800.

3.3. Grid sensitivity study

In order to determine the appropriate element size of the wind turbine surface, the grid sensitivity is studied. The wind speed and speed are set to the rated wind speed and speed of NREL 5MW wind turbine, namely 11.4m/s and 1.267rad/s. The dimensions of six grid surfaces on the surface of the wind turbine are studied, namely 0.095m, 0.1m, 0.11m, 0.125m, 0.15m, and 0.2m. The relevant total number of grids and the calculated wind turbine torque are shown in Table 2 and Figure 4. The wind turbine torque converges at 0.1m of the grid size of the wind turbine surface. The grid size further refined to 0.095m only achieves a relative difference of 0.7%, but it increases the total number of grids from 10.2 million to 11.9 million, which significantly increases the time cost. Considering the calculation time and accuracy, in this paper, the mesh size of 0.1m is considered as the appropriate element surface size for CFD modeling of wind turbine model surface.

Table 2: Results of mesh sensitivity analysis

	Wind rotor simulation					
Mesh size	0.095m	0.1m	0.11m	0.125m	0.15m	0.2m
Rotor torque(Nm)	4152255	4121922	4057981	3860110	3692010	3185126
Number of meshes	11952036	10207261	8690368	6967765	5382168	3220948

ISSN 2706-655X Vol.5, Issue 3: 16-25, DOI: 10.25236/IJFET.2023.050304

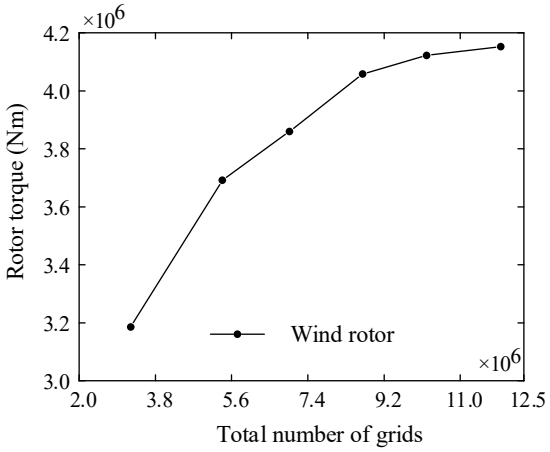

Figure 4: Torque convergence diagram of wind turbine

4. Calculation results and discussion

4.1. Flow field analysis of wind turbine

Figures 5 (a) ~ (c) are the wind speed distribution nephogram of blade root fracture, blade middle fracture and blade tip fracture at 6m in front of the wind turbine. The wind speed is greatly affected in the area directly opposite the plane of the wind wheel. There are low wind speed concentration areas in the sweep area of the three blades. The closer the blade is, the lower the wind speed is. Among them, the wind wheel area with broken blade tip has a large concentration area of low wind speed, which indicates that it absorbs more wind energy, resulting in lower wind speed. Figures 5 (d) ~ (f) are the velocity distribution nephogram at 2 meters in front of the wind turbine. It is obvious that the low wind speed area near the blade projection of the wind turbine is more obvious. In addition, it is also found that in the periphery of the low wind speed concentration area, there are local high wind speed areas with a divergence trend. The wind turbine has disturbance phenomenon at the blade fracture position, among which the disturbance caused by the blade root fracture is the smallest and the disturbance caused by the blade tip fracture is the largest. Figures 5 (g) ~ (i) show the wind speed nephogram at the wind wheel plane. The high wind speed area of the complete blade extends from the root to the tip and the wind speed disturbance area caused by the tip sweep; The same phenomenon exists for the broken blades, and the high wind speed area extends to the broken section. The tail of the broken blade will also disturb the flow field. Compared with the tip disturbance of the complete blade, the influence of the tip disturbance is smaller. As the position of the broken blade develops from the root to the tip, the disturbance gradually increases until it is close to the disturbance of other blades. This is because the broken blade is within the influence range of the flow field of the previous blade, and the high wind speed region caused by the disturbance of the broken blade tail will be partially offset.

Figures 6 (a) ~ (c) are the wind speed nephogram at 2 meters behind the plane of the wind wheel. The speed distribution is similar to that at the plane of the wind wheel, which is greatly affected by the rotation of the wind wheel. Figures 6 (d) ~ (f) are the velocity distribution nephogram at 6 meters behind the wind wheel. At this time, the wind wheel gradually separated from the influence of blade rotation, forming a low wind speed point area at the center of the wind wheel, and then a circle of high wind speed areas around the low wind speed point area, and at the periphery of the high wind speed area is the low wind speed area. Figures 6 (g) ~ (i) are the wind speed nephogram at 10m behind the wind wheel. At this time, in the flow field, the influence of the rotation effect of the wind wheel is weakened, the range of the high wind speed area gradually diffuses to the outside of the wind wheel, and the effect of the blade sweeping is basically invisible, and the low wind speed area after the blade sweeping range gradually joins together. From the range of low wind speed area, with the gradual completion of the blade, the low wind speed area slowly becomes circular and keeps balance. This also reflects that when the blade fracture occurs at the root of the blade, the imbalance of the wind wheel will be aggravated, leading to a large sudden change in the stress load, leading to serious accidents, so the wall root fracture should occur.

ISSN 2706-655X Vol.5, Issue 3: 16-25, DOI: 10.25236/IJFET.2023.050304

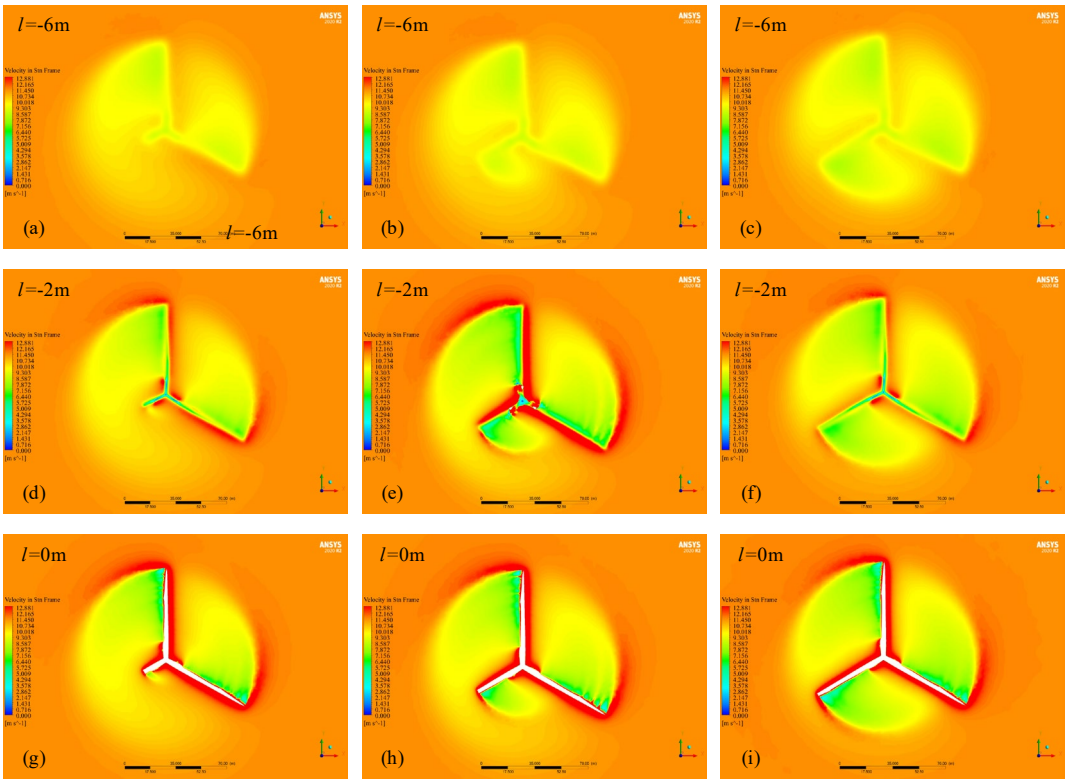

Figure 5: Flow field of the wind turbine from 6m in front of the wind turbine to the plane of the wind turbine

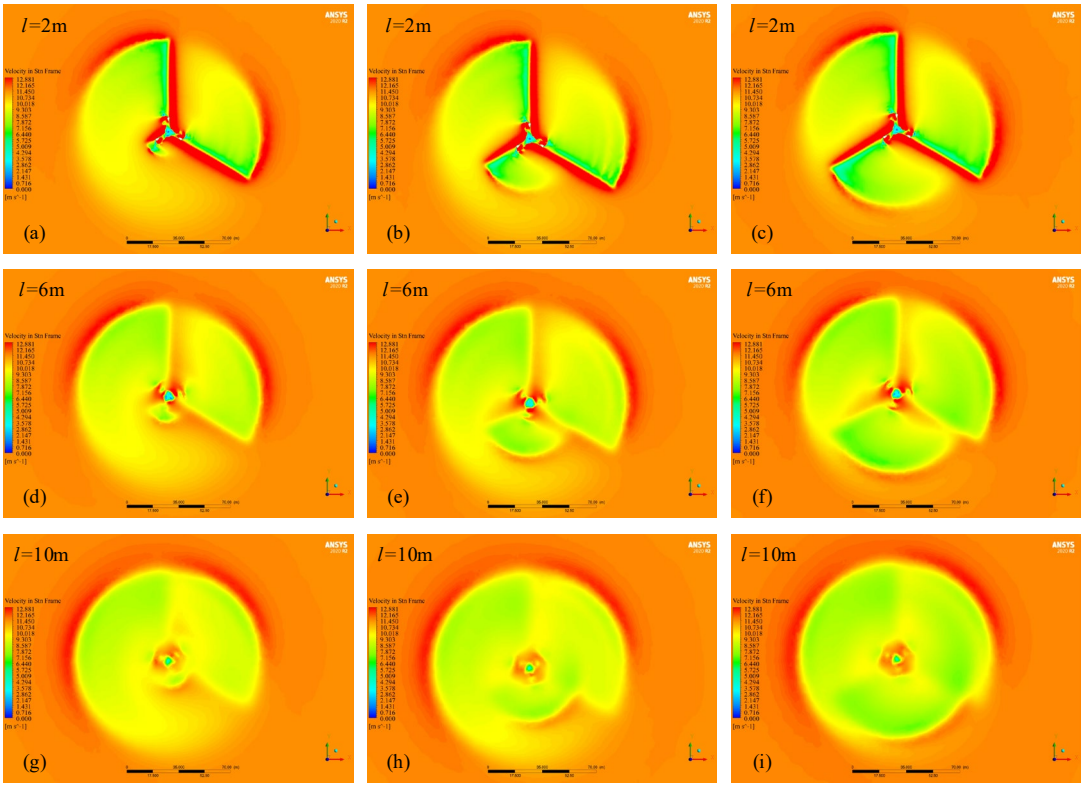

Figure 6: Flow field of wind turbine from 2m to 10 behind the wind turbine

4.2. Analysis of surface pressure and streamline distribution of wind turbine

Figure 7 shows the streamline and pressure contour of the front and back sides of the wind turbine when the fault occurs at different locations, with the pressure range of - 5500Pa~2500Pa. As shown in the figure, from the blade root, the pressure on the leeward side of the wind turbine gradually decreases

ISSN 2706-655X Vol.5, Issue 3: 16-25, DOI: 10.25236/IJFET.2023.050304

until a large area of negative pressure area appears at the blade tip. The pressure on the windward side gradually increases from the blade root, and the pressure difference between the windward side and the leeward side at the blade tip is the largest, which is conducive to the improvement of the aerodynamic force at the blade tip. From the streamline distribution on the surface of the wind turbine, it can be found that there is obvious flow separation phenomenon in the blade root area, which is because the rotation speed of the blade root is the minimum, the angle of attack of the incoming flow is increased, and the flow separation is serious. The flow separation on the broken blade moves towards the blade tip with the integrity of the blade.

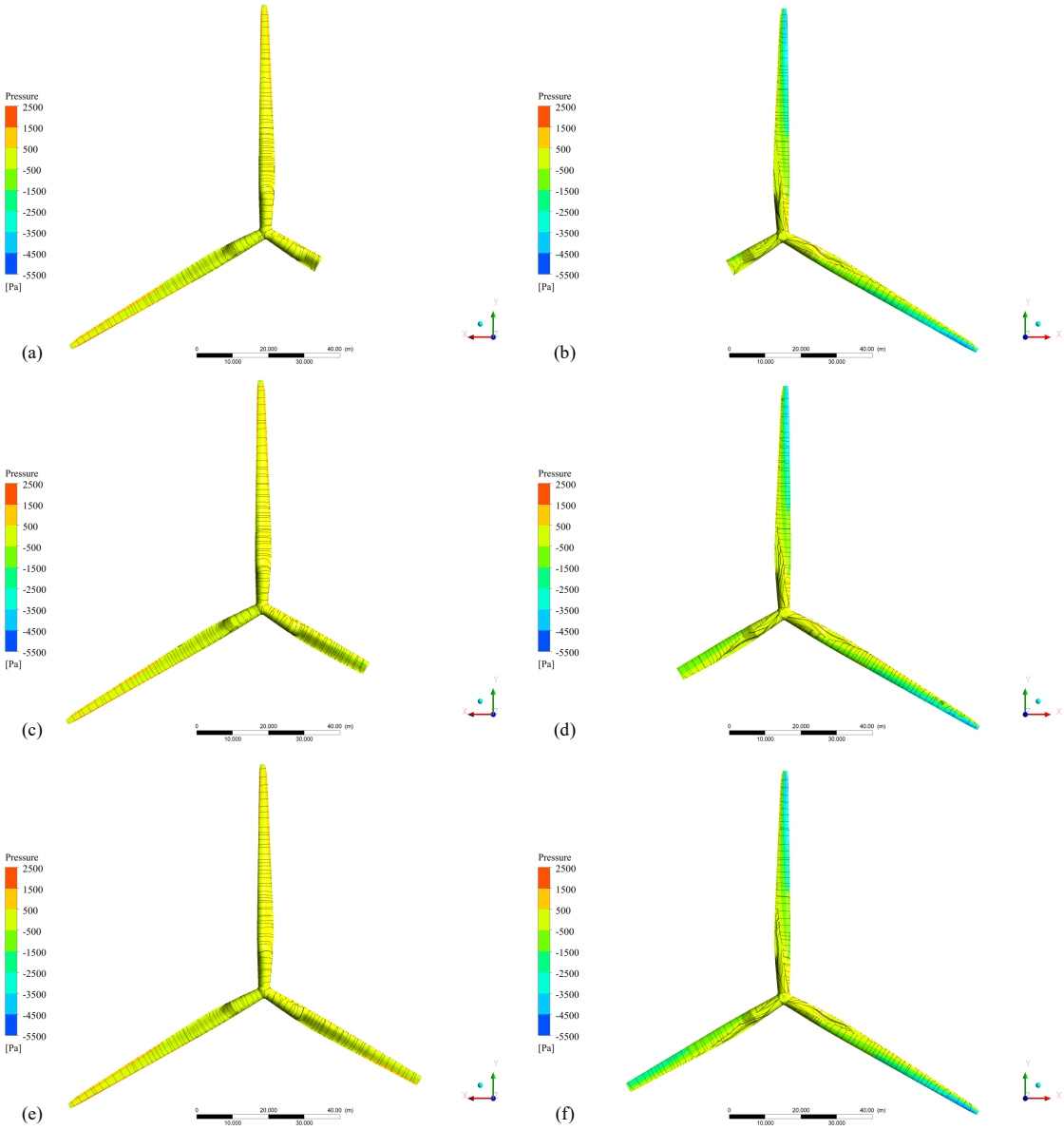

Figure 7: Surface streamline and pressure distribution of wind turbine under different fracture accidents

4.3. Torque and thrust under flying condition

Figure 8 shows the thrust and torque curve when the blade breaks after the blade galloping, Figure 8 (a) and Figure 8 (b) show the blade root fracture, Figure 8 (c) and Figure 8 (d) show the blade middle fracture, and Figure 8 (e) and Figure 8 (f) show the blade tip fracture. It can be found that the trend of thrust curve changing with the speed of the flying car at different fracture positions is consistent, which is rising with the speed of the flying car. In the torque curve, the blade root fracture and the blade tip fracture have the same trend, both of which decrease with the increase of the speed. Only when the middle of the blade breaks, the torque first rises and then decreases. This may be due to the change of the wind

ISSN 2706-655X Vol.5, Issue 3: 16-25, DOI: 10.25236/IJFET.2023.050304

energy utilization coefficient at the time of the middle fracture, resulting in the backward movement of the best tip speed ratio. Through the analysis of aerodynamic loads, it can be learned that once a runaway occurs, the thrust will rise sharply, which will bring huge loads to the wind turbine, and even lead to the collapse of the wind turbine. Therefore, once there is a strong typhoon, the downpour should be stopped in time to prevent accidents.

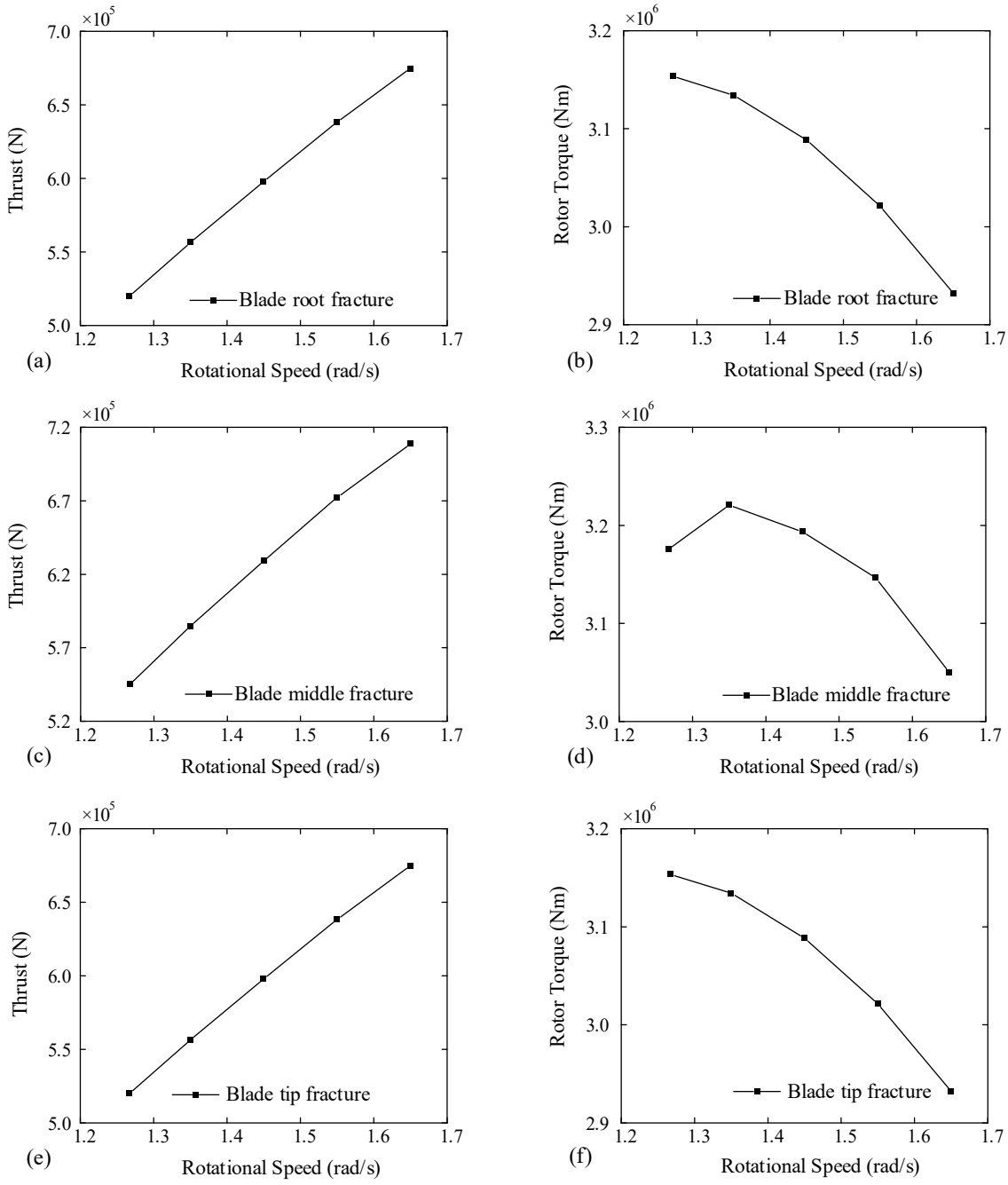

Figure 8: Torsion and thrust of runaway after blade fracture

5. Conclusion

This paper mainly introduces the division of blade fracture in blade fracture accident, and the simulation analysis of wind turbine blade fracture accident. The simulation results were compared and analyzed with the flow field velocity nephogram of the wind turbine rotor at different fracture locations. It was found that with the deepening of the fracture degree, the flow field became more unbalanced, and it was necessary to prevent the occurrence of blade fracture accidents. The pressure distribution and streamline on the blade surface are also analyzed. It is found that the tip position is the part with the

ISSN 2706-655X Vol.5, Issue 3: 16-25, DOI: 10.25236/IJFET.2023.050304

largest pressure difference on the blade surface, and obvious flow separation occurs at the blade root attachment. As the fracture position is farther away from the blade root, the flow separation range near the blade root shifts to the blade root. The aerodynamic load of the wind turbine at different speed is also analyzed. It is found that in extreme wind weather such as typhoon, once the emergency pitch fails, the sudden sudden strong wind will cause the wind turbine to fly. At this time, the axial thrust and torque of the wind turbine will increase with the increase of speed. Therefore, in order to prevent the phenomenon of flying, the pitch system should be checked and maintained regularly.

References

[1] Chou J-S, Ou Y-C, Lin K-Y, et al. Structural failure simulation of onshore wind turbines impacted by strong winds [J]. Engineering Structures, 2018, 162: 257-269.
[2] Chen X, Xu J Z. Structural failure analysis of wind turbines impacted by super typhoon Usagi [J]. Engineering Failure Analysis, 2016, 60: 391-404.
[3] Juchuan Dai. Dynamic characteristics analysis of direct-drive wind turbine under blade fracture accident [J]. Journal of Mechanical Engineering, 2013, 49(02): 190-198.
[4] Han Lu, Yu Xiangtian, Wang Ying, etc Cause analysis of fan blade fracture [J]. Aerospace material technology, 2017, 47(01): 67-71.
[5] He Jianwu, Liu Chao, Zhang Zhengchuan, et al. Analysis of transient stress characteristics of wind turbine generator unit in case of blade failure [J]. wind energy source, 2017, (09): 58-63.
[6] Gu Yongqiang, Feng Jinfei, Jia Baohua, et al Analysis of the influence of wind turbine blade breaking on blade dynamics [J]. Inner mongolia electric power, 2020, 38(05): 1-4.
[7] Menter F R J A j. Two-equation eddy-viscosity turbulence models for engineering applications [J]. 1994, 32(8): 1598-1605.
[8] Menter F R, Kuntz M, Langtry R J T, heat, et al. Ten years of industrial experience with the SST turbulence model [J]. 2003, 4(1): 625-632.
[9] J. Jonkman S B, W. Musial, G. Scott. Definition of a 5-MW Reference Wind Turbine for Offshore System Development [J]. National Renewable Energy Lab(NREL), Golden, CO (United States), 2009.
[10] Wang L, Quant R, Kolios A. Fluid structure interaction modelling of horizontal-axis wind turbine blades based on CFD and FEA [J]. Journal of Wind Engineering and Industrial Aerodynamics, 2016, 158: 11-25.
[11] Ji B, Zhong K, Xiong Q, et al. CFD simulations of aerodynamic characteristics for the three-blade NREL Phase VI wind turbine model [J]. Energy, 2022, 249.
[12] Eltayesh A, Castellani F, Burlando M, et al. Experimental and numerical investigation of the effect of blade number on the aerodynamic performance of a small-scale horizontal axis wind turbine [J]. Alexandria Engineering Journal, 2021, 60(4): 3931-3944.